Egyptian Journal of Radiology and Nuclear Medicine

RESEARCH

Open Access

The effects of anatomical location and distance from dental implants on the quality and quantity of metal artifacts in cone beam computed tomography scans: a cross-sectional study

Yalda Salari[1], Shirin Sakhdari[2], Ladan Hafezi[2], Faeze Zare Bidoki[2] and Seyed Ali Mosaddad[3,4*]

Abstract

Background Artifacts in cone beam computed tomography (CBCT) images can cause disruptions in diagnosis and treatment. Multiple factors influence the artifacts, including the quality and technology of devices, positions, patient-related factors, device settings, and bone density. Besides, anatomical area and distance from the implant affect the artifacts. This study aimed to investigate the effects of anatomical location and distance from the implant on the quality and quantity of artifacts.

Methods A total of 200 CBCT images of patients with titanium implants and prostheses in the anterior and posterior regions of the maxilla and mandible were evaluated in this study. Four areas were assessed for each implant in three apical, middle, and cervical regions with distances of 3 mm, 4 mm, and 5 mm from the implant. Besides, the impact of adjacent implants on the artifacts was investigated. An ANOVA test with post hoc Bonferroni correction was used to analyze variable differences between subgroups.

Results The differences were statistically significant, except for the difference between the posterior areas of the upper and lower jaws. A comparison of different areas revealed that most artifacts were related to the anterior maxilla, followed by anterior mandibular regions. The results of covariance analysis indicated that region and location had independent effects on the amount of artifacts.

Conclusions Artifacts are more frequent in the anterior region compared to the posterior site. They are also more frequent in the maxilla than the mandible and cervical areas close to the implant than the middle and apical regions.

Keywords Artifacts, Metal implants, CBCT

Background

The first cone beam computed tomography (CBCT) apparatus was the NewTom 9000 (Quantitative Radiology, Verona, Italy), designed in 1998 for maxillofacial imaging [1]. Since then, there has been rapid progress in generating CBCT units for imaging the maxillofacial area. In dentistry, CBCT yields 3D images that are more useful than conventional tomography due to more straightforward image acquisition and lower radiation doses [2–4]. A tomography scan is performed using a cone-shaped X-ray beam emission in a 360-degree rotation; the complete structure volume can be captured.

*Correspondence:
Seyed Ali Mosaddad
mosaddad.sa@gmail.com
Full list of author information is available at the end of the article

The images are reconstructed in a computer system bi-dimensionally, three-dimensionally, and volumetrically [5].

Effective dental implant rehabilitation requires post-operative assessment and accurate preoperative surgical planning. In implantology, linear assessments of height and depth increase immunity and provide novel opportunities in oral rehabilitation. CBCT facilitates the remaining bone quantification and the precise localization of anatomical structures [6]. Although CBCT images have several advantages, they also have some limitations, including the formation of image artifacts, which is their most common disadvantage [7]. Generally, an image artifact represents a structure near an image, which is produced based on reconstruction data and does not correspond to the actual features of the evaluated object [8, 9]. It is known that gray-level non-uniformities result in artifact generation in reconstructed CBCT images, which can simulate obscure results similar to pathologies [7].

Artifacts have different origins, associated with variations between the physical features of an object and its attenuation coefficient delivered by the detector, besides the CBCT unit limitations, such as features of the mathematical algorithm in retroprojections used for image reconstruction. Also, object positioning and composition in the field of view (FOV) can disrupt this process [10, 11]. Moreover, patients may cause artifacts because of the presence of materials in the examination region and movements during image acquisition. On the contrary, reconstruction artifacts are related to errors in the reconstruction of obtained sections [12, 13].

For a better understanding, artifacts are divided based on factors related to their origin. The primary artifacts include motion artifacts, helical artifacts, ring artifacts, artifacts produced by highly dense materials, scatter artifacts, beam-hardening artifacts, scattering artifacts, pseudo-enhancement, noise artifacts, metal artifacts, extinction artifacts, and cone beam effect artifacts [7, 12]. Images are susceptible to artifacts in the presence of metals, such as dental implants and metallic restorations in the scanning region. Occasionally, metal artifacts result in unusable images. It has been reported that beam-hardening artifacts, streaking artifacts, and band-like radiolucent areas are the most common artifacts surrounding the implants, possibly affected by the implant material, distance, evaluated sites, bone type, FOV size, CBCT type, kilovoltage peak (kVp), milliamperage (mA), and voxel size [6].

Several studies have investigated the factors mentioned above that can contribute to forming artifacts in CBCT images [9, 14–16]. However, previous studies demonstrated some limitations, and their reporting was inconclusive. For example, the study by Machado et al. [11] sought to quantitatively assess metal artifacts from implants in various maxillomandibular locations using CBCT images. However, their study included implants of different lengths and diameters, which could have affected the results. Another study by Farhangnia et al. [14], which only included mandibular implants, fell short of thoroughly evaluating all anatomical locations of implants placed within jaws. Therefore, the current study aimed to assess the quantity and quality of metal artifacts in CBCT images produced by similar dental implants in the anterior and posterior regions of the maxilla and mandible. The null hypothesis was that the location of the placed implants would significantly affect the generation of artifacts.

Methods

This cross-sectional study was performed at the School of Dentistry of Islamic Azad University, Tehran, Iran. Our institutional research ethics committee approved this study (No.: IR.IAU.DENTAL.REC.1399.090), and all participants' written informed consent was obtained. This study examined the CBCT images of patients with titanium implants and prostheses in different areas of the maxilla and mandible (anterior and posterior areas). All images were analyzed in four implant locations within the jaws and at three different sections of each implant. Besides, the effect of "adjacent implants" on the artifacts was evaluated.

The sample size was calculated based on previous studies [11] and the number of study variables. The required sample size was calculated using the following formula $n = \frac{(Z_\alpha + Z_\beta)^2 P(1-P)}{e^2}$, in which e is the level of precision, P is the desired proportion in the population, and Z is the value corresponding to the area under the standard normal curve. Therefore, considering $\alpha = 5\%$, $\beta = 10\%$, ($Z = 3.24$), $P = 80\%$, and $e = 10\%$, the minimum sample size was 168 implants (42 implants in each group).

Patients who were referred to the respective faculty of the university from September 2021 to September 2022 for a new dental implant surgery and already had other dental implants placed in their jaw were the candidates to participate in this study. Four study groups were considered in this investigation: Group 1: patients who had implants in the anterior maxilla; Group 2: patients who had implants in the posterior maxilla; Group 3: patients who had implants in the anterior mandible; and Group 4: patients who had implants in the posterior mandible. The anterior implants referred to implants in the canine and incisor teeth, and the posterior implants referred to implants in the premolars and posterior area [11, 17, 18]. The sampling was conducted using the convenience sampling method until the sample size reached 50 implants in each group (n total = 200 implants).

CBCT images were acquired using a Kodak 9500 3D CBCT system (Carestream Health, Rochester, NY) and based on an established acquisition protocol [19]: voxel size, 0.180 mm^3; mA, 10 mA; voltage, 90 kVp; grayscale, 16 bits; exposure time, 11 s, and FOV, 10×10 cm^2. The scan parameters and protocol adhered to the radiation protection principle of justification [20]. All patients wore a lead apron to protect the body trunk. Inclusion criteria comprised (1) partially edentulous patients, (2) of any sex and (3) age (above 18 years old), (4) having bone-level dental implants, all from the same brand, model, and dimension, (5) in any maxillary or mandibular regions (6) loaded with prosthetic restorations (all with titanium abutments and cemented porcelain-fused-to-metal restorations) at the time of examination. The exclusion criteria were as follows: (1) zygomatic implants, (2) implants without restorations, (3) implants in an area that received bone grafts previously, (4) implants adjacent to endodontically treated teeth (with/without metallic intracanal posts), or (5) adjacent to teeth restored with amalgam fillings or prosthetic crowns.

The acquired images were analyzed using the OnDemand 3D Dental software (Cybermed, Seoul, Korea) and reported as maximum/minimum values and mean ± standard deviation (SD). The CBCT images were then divided into three subgroups. (I) Based on implant positioning: isolated or adjacent to other implants. The adjacent implants included implants with a maximum inter-implant distance of 5 mm [11]. (II) Based on the cross section along the implant length, which included each image's apical, middle, and cervical regions. The axial images were reconstructed for each implant in the apical, middle, and cervical cross sections, and they were examined for the grayscale value (GSV) (Fig. 1a–d). The apical section represents an area that enables the examiner to assess the entire diameter of the implant. In contrast, the cervical area represents an area where the examiner can view the whole diameter of the implant before the prosthetic connection. For each implant, the middle section was midway between the apical and cervical images. (III) Based on the distance from the implants' platform: the GSV was assessed around each implant in the apical, middle, and cervical areas at three distances of 3 mm, 4 mm, and 5 mm from the implant platform (Fig. 2). The entire grouping is graphically represented in Fig. 3. The region of interest (ROI) was drawn as circles with a center congruent with the implant center and a radius placed at 3-, 4-, and 5-mm distances from the implant platform, using the ROI tool of the OnDemand software in the three cross sections of the implants mentioned above. This region covered the entire implant area and the surrounding bone. Following the technique presented by Pauwels et al. [19], the artifacts found in each chosen ROI were counted. A histogram tool was used to determine the maximum and minimum gray values, which were used to estimate the actual standard deviation (SD), carried out in Microsoft Excel (ver. 2010, Windows 10, Microsoft, USA). As a constant value, the maximum theoretical standard deviation depends on the scanner type. The images created using the CBCT scanner utilized in the present investigation are of a 16-bit scale (65,536 Gy values). Given the same value, the maximum theoretical standard deviation, which corresponds to half the gray values of a 16-bit image, was determined (32,768 values). Based on the study by Pauwels et al. [19], the quantification of artifacts can be defined as actual standard deviation/theoretical maximum standard deviation × 100. As a result, the actual standard deviation was transformed into a percentage of the maximum theoretical standard deviation, in which higher percentages are rendered as artifacts with more prominence. To assess the method's reproducibility, all scans were reviewed by two oral and maxillofacial radiologists twice, separated by two weeks.

The mean values of artifacts were compared between the groups using the ANOVA test. The Bonferroni test was also used for pairwise comparisons between the subgroups. To lower the possibility of a false positive, statisticians employ the Bonferroni test, which is an adjustment to ensure that data would not falsely appear as statistically significant. ANCOVA was also applied to evaluate the independent effects of implant position and region on the amount of artifacts. The level of statistical significance was set at 0.05. The Wilcoxon signed-rank test was also performed to assess paired nonparametric data regarding adjacency to the implant. The intra- and inter-class correlation coefficients (ICC) were computed to evaluate the intra-observer and inter-observer agreements.

Results

This study examined 200 CBCT scans from 200 patients with 200 placed implants further classified into four main groups based on the placed area in the maxilla or mandible (n each group = 50) and into subgroups II ($n = 3$; apical, middle, cervical) and III ($n = 3$; distances: 3, 4, and 5 mm); therefore, in total, 1800 radiographic assessments (200 total × 3 subgroup II × 3 subgroup III) were performed in this study. Also, 450 samples (50 in each leading group × 3 subgroup II × 3 subgroup III) were evaluated regarding anterior or posterior locations within jaws. The mean values of artifacts in each group are presented in Table 1. The highest and lowest mean ± SD amount of artifacts (gray value) were observed in the cervical region at 3 mm (4773.224 ± 1428.128) and in the apical region at 5 mm (1832.190 ± 694.467), respectively.

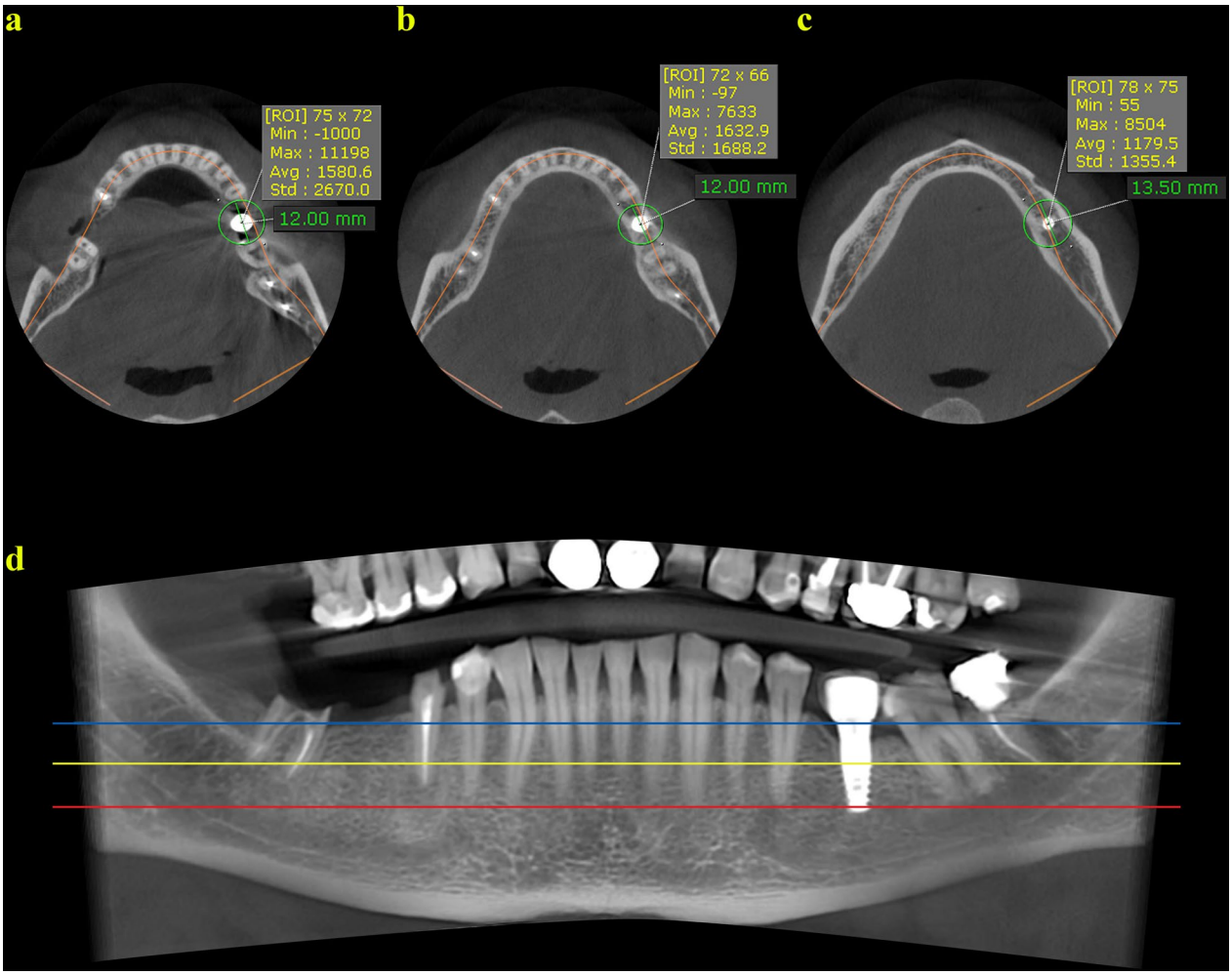

Fig. 1 Grayscale value at the **a** cervical region (**d**-blue line; the most cervical zone that permitted a view of the implant's whole diameter directly below the prosthetic connection), at the **b** middle region (**d**-yellow line; the area in the center of the previously chosen cervical and apical parts for each specific implant), and at the **c** apical region (**d**-red line; the most apical cross section that enabled visualization of the total implant diameter) of a four-millimeter diameter implant with a peri-implant perimeter having 12 mm diameter (at a 4 mm distance from the implant platform; green circle)

As shown in Table 2, a comparison of different conditions based on the Bonferroni test indicated that the observed differences for various distances were statistically significant, suggesting the impact of distance from the implant on the artifacts. The significant differences are shown in Table 2.

To determine the region's impact, the apical, middle, and cervical areas were compared at different distances and categorized based on their 95% confidence intervals (CIs), as shown in Fig. 4.

As shown in Table 3, most artifacts were found in the maxilla, followed by the anterior region of the mandible. The highest and lowest mean ± SD amount of artifacts (gray value) based on maxillomandibular locations were observed in the anterior maxilla, 3720.090 ± 1515.5030, and the posterior maxilla, 2612.258 ± 2833.5081. According to Fig. 5, the results of the Bonferroni test at 95% CIs indicated significant differences between all evaluated regions except for the posterior areas of the jaws. In other words, posterior samples showed fewer artifacts; the maxilla had more artifacts among anterior samples. The analysis of covariance showed that area (cervical, middle, and apical) and position (anterior vs. posterior and upper vs. lower jaw) had independent effects on the amount of artifacts ($F = 16.9$ and $F = 36.5$, respectively; $P < 0.0001$ for both).

There were 20 specimens of adjacent implants in this study. The analysis of mean artifacts related to adjacent implants showed that the mean value of pairs was not significantly different. As the mean distribution of

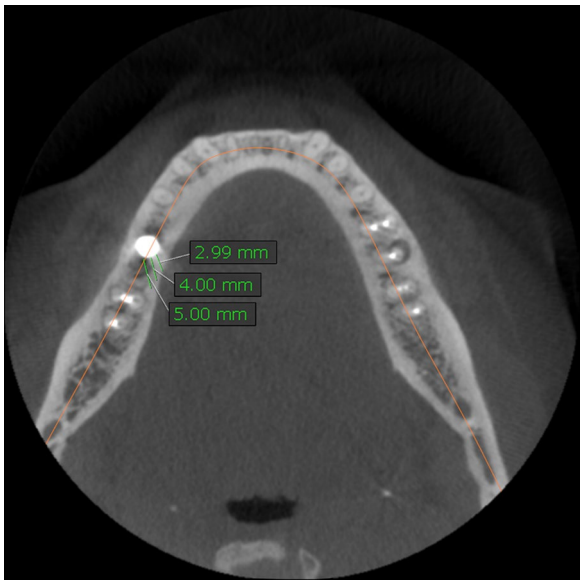

Fig. 2 Three distances, 3-, 4-, and 5-mm from the implant platform, were used to evaluate the grayscale value around each implant at the apical, middle, and cervical sections

data was not normal in one of the groups, the Wilcoxon signed-rank test was applied, which indicated the same results ($P=0.71$). Moreover, the correlation of sample means was very weak in the adjacent implants ($r=0.27$, $P=0.24$). Therefore, the amount of artifacts was related to location, although it was not significantly affected by the presence of adjacent implants. As shown in Table 4, the mean values of adjacent pairs were not significantly different. In our study, the intra- and inter-observer agreements were 96% and 92%, respectively. These results demonstrated both high and excellent inter- and intra-examiner reliability.

Discussion

The current study was performed to quantitatively and qualitatively evaluate metal artifacts in the anterior and posterior areas of the maxilla and mandible generated by dental implants in CBCT images. Based on the results of data analysis in the present study, the null hypothesis was accepted. There were more artifacts at a 3-mm distance from implants compared to 4-mm and 5-mm distances in all anatomical locations (cervical, middle, and apical areas). In other words, maintaining distance from metal implants can reduce the artifacts' rate and the mean gray value. Also, artifacts were more frequent in the anterior and upper jaw than in the posterior and lower jaw areas. The results of the ANCOVA test showed that the orientation and location of metal implants independently affected the rate of artifacts ($P<0.0001$). A comparison of nine positions revealed that the highest rate of artifacts was related to

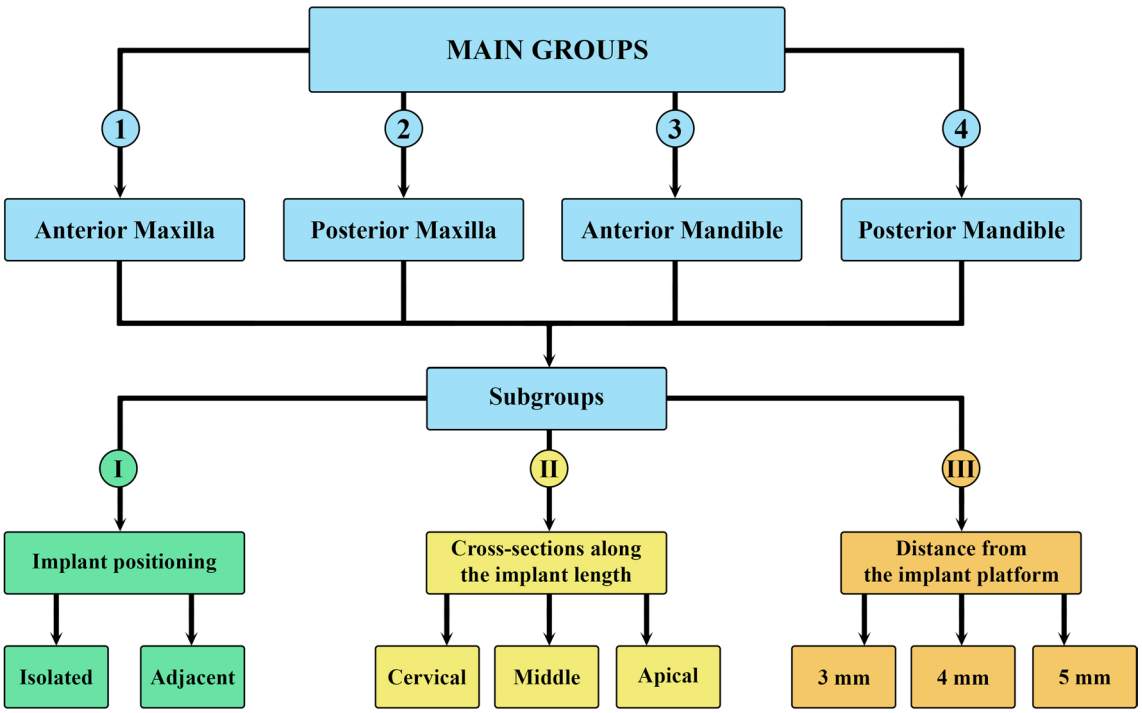

Fig. 3 A graphical illustration demonstrating the main study groups and subgroups

Table 1 Mean ± SD of GSV in 36 groups based on the position/area

Type	Area	The mean amount of artifacts (gray value)	SD	95% Confidence interval	
				Lower bound	Upper bound
Apical 3 mm	Posterior maxilla	2484.280	928.819	1956.746	3011.814
	Anterior maxilla	4090.540	1656.242	3563.006	4618.074
	Posterior mandible	3449.926	4505.080	2922.392	3977.460
	Anterior mandible	3970.114	1321.717	3442.580	4497.648
Apical 4 mm	Posterior maxilla	2154.916	758.817	1627.382	2682.450
	Anterior maxilla	3397.960	1323.594	2870.426	3925.494
	Posterior mandible	2458.284	1227.996	1930.750	2985.818
	Anterior mandible	3305.072	1014.564	2777.538	3832.606
Apical 5 mm	Posterior maxilla	1832.190	694.467	1304.656	2359.724
	Anterior maxilla	3061.700	1369.162	2534.166	3589.234
	Posterior mandible	2061.920	950.271	1534.386	2589.454
	Anterior mandible	2395.926	875.911	1868.392	2923.460
Cervical 3 mm	Posterior maxilla	4175.148	5702.986	3647.614	4702.682
	Anterior maxilla	4773.224	1428.128	4245.690	5300.758
	Posterior mandible	3078.364	1284.139	2550.830	3605.898
	Anterior mandible	4220.300	1092.704	3692.766	4747.834
Cervical 4 mm	Posterior maxilla	2459.726	746.228	1932.192	2987.260
	Anterior maxilla	4142.306	1582.835	3614.772	4669.840
	Posterior mandible	2932.476	1598.341	2404.942	3460.010
	Anterior mandible	3313.258	1044.744	2785.724	3840.792
Cervical 5 mm	Posterior maxilla	2359.878	2603.755	1832.344	2887.412
	Anterior maxilla	3531.520	1402.338	3003.986	4059.054
	Posterior mandible	2361.592	1710.237	1834.058	2889.126
	Anterior mandible	3253.458	1415.138	2725.924	3780.992
Middle 3 mm	Posterior maxilla	3753.606	5062.234	3226.072	4281.140
	Anterior maxilla	3881.440	1242.308	3353.906	4408.974
	Posterior mandible	2843.720	871.733	2316.186	3371.254
	Anterior mandible	3658.500	981.120	3130.966	4186.034
Middle 4 mm	Posterior maxilla	2330.520	742.143	1802.986	2858.054
	Anterior maxilla	3445.700	1293.833	2918.166	3973.234
	Posterior mandible	2356.752	728.145	1829.218	2884.286
	Anterior mandible	3186.812	1003.974	2659.278	3714.346
Middle 5 mm	Posterior maxilla	1960.060	578.727	1432.526	2487.594
	Anterior maxilla	3156.420	1575.284	2628.886	3683.954
	Posterior mandible	2208.320	1195.989	1680.786	2735.854
	Anterior mandible	2563.174	995.042	2035.640	3090.708

the cervical position, while the apical and middle areas showed similar rates of artifacts. The pairwise comparison of different positions revealed that these differences were primarily significant. Overall, the anterior part of the upper jaw accounted for the highest rate of artifacts, followed by the anterior part of the lower jaw. On the other hand, the posterior areas of the upper and lower jaws were comparable, without any significant differences.

In a study in 2018, Machado et al. [11] conducted an experiment using the same methodology as the present study. They analyzed CBCT images to quantitatively compare metal artifacts caused by implants in various maxillomandibular areas (anterior maxilla, posterior maxilla, anterior mandible, and posterior mandible). Similar to our findings, the anterior areas generated most artifacts compared to the posterior regions. The cervical region was most affected by artifacts, and there was no discernible difference in the quantity of generated

Table 2 Comparison of different sectional regions (apical, middle, cervical) and their relationships

Multiple Comparisons						
Dependent Variable: Average						
Bonferroni						
(I) Type	**(J) Type**	**The mean difference of the artifacts amount (gray value) (I–J)**	**Standard error**	**Sig**	**95% Confidence interval**	
					Lower bound	**Upper bound**
Apical 3 mm	Apical 4 mm	669.657*	190.191	.016	60.658	1278.656
	Apical 5 mm	1160.781*	190.191	.000	551.782	1769.780
	Cervical 3 mm	−563.044	190.191	.112	−1172.043	45.955
	Cervical 4 mm	286.774	190.191	1.000	−322.226	895.773
	Cervical 5 mm	622.103*	190.191	.039	13.104	1231.102
	Middle 3 mm	−35.602	190.191	1.000	−644.601	573.398
	Middle 4 mm	668.769*	190.191	.016	59.770	1277.768
	Middle 5 mm	1026.721*	190.191	.000	417.722	1635.721
Apical 4 mm	Apical 3 mm	−669.657*	190.191	.016	−1278.656	−60.658
	Apical 5 mm	491.124	190.191	.356	−117.875	1100.123
	Cervical 3 mm	−1232.701*	190.191	.000	−1841.700	−623.702
	Cervical 4 mm	−382.883	190.191	1.000	−991.883	226.116
	Cervical 5 mm	−47.554	190.191	1.000	−656.553	561.445
	Middle 3 mm	−705.258*	190.191	.008	−1314.258	−96.259
	Middle 4 mm	−.888	190.191	1.000	−609.887	608.111
	Middle 5 mm	357.065	190.191	1.000	−251.935	966.064
Apical 5 mm	Apical 3 mm	−1160.781*	190.191	.000	−1769.780	−551.782
	Apical 4 mm	−491.124	190.191	.356	−1100.123	117.875
	Cervical 3 mm	−1723.825*	190.191	.000	−2332.824	−1114.826
	Cervical 4 mm	−874.007*	190.191	.000	−1483.007	−265.008
	Cervical 5 mm	−538.678	190.191	.168	−1147.677	70.321
	Middle 3 mm	−1196.383*	190.191	.000	−1805.382	−587.383
	Middle 4 mm	−492.012	190.191	.351	−1101.011	116.987
	Middle 5 mm	−134.059	190.191	1.000	−743.059	474.940
Cervical 3 mm	Apical 3 mm	563.044	190.191	.112	−45.955	1172.043
	Apical 4 mm	1232.701*	190.191	.000	623.702	1841.700
	Apical 5 mm	1723.825*	190.191	.000	1114.826	2332.824
	Cervical 4 mm	849.818*	190.191	.000	240.818	1458.817
	Cervical 5 mm	1185.147*	190.191	.000	576.148	1794.146
	Middle 3 mm	527.443	190.191	.202	−81.557	1136.442
	Middle 4 mm	1231.813*	190.191	.000	622.814	1840.812
	Middle 5 mm	1589.766*	190.191	.000	980.766	2198.765
Cervical 4 mm	Apical 3 mm	−286.774	190.191	1.000	−895.773	322.226
	Apical 4 mm	382.883	190.191	1.000	–226.116	991.883
	Apical 5 mm	874.007*	190.191	.000	265.008	1483.007
	Cervical 3 mm	−849.818*	190.191	.000	−1458.817	−240.818
	Cervical 5 mm	335.330	190.191	1.000	−273.670	944.329
	Middle 3 mm	−322.375	190.191	1.000	−931.374	286.624
	Middle 4 mm	381.996	190.191	1.000	−227.004	990.995
	Middle 5 mm	739.948*	190.191	.004	130.949	1348.947

Table 2 (continued)

Multiple Comparisons						
Dependent Variable: Average						
Bonferroni						
(I) Type	**(J) Type**	**The mean difference of the artifacts amount (gray value) (I–J)**	**Standard error**	**Sig**	**95% Confidence interval**	
					Lower bound	**Upper bound**
Cervical 5 mm	Apical 3 mm	−622.103*	190.191	.039	−1231.102	−13.104
	Apical 4 mm	47.554	190.191	1.000	−561.445	656.553
	Apical 5 mm	538.678	190.191	.168	−70.321	1147.677
	Cervical 3 mm	−1185.147*	190.191	.000	−1794.146	−576.148
	Cervical 4 mm	−335.330	190.191	1.000	−944.329	273.670
	Middle 3 mm	−657.704*	190.191	.020	−1266.704	−48.705
	Middle 4 mm	46.666	190.191	1.000	−562.333	655.665
	Middle 5 mm	404.619	190.191	1.000	−204.381	1013.618
Middle 3 mm	Apical 3 mm	35.602	190.191	1.000	−573.398	644.601
	Apical 4 mm	705.258*	190.191	.008	96.259	1314.258
	Apical 5 mm	1196.383*	190.191	.000	587.383	1805.382
	Cervical 3 mm	−527.443	190.191	.202	−1136.442	81.557
	Cervical 4 mm	322.375	190.191	1.000	−286.624	931.374
	Cervical 5 mm	657.704*	190.191	.020	48.705	1266.704
	Middle 4 mm	704.371*	190.191	.008	95.371	1313.370
	Middle 5 mm	1062.323*	190.191	.000	453.324	1671.322
Middle 4 mm	Apical 3 mm	−668.769*	190.191	.016	−1277.768	−59.770
	Apical 4 mm	.888	190.191	1.000	−608.111	609.887
	Apical 5 mm	492.012	190.191	.351	−116.987	1101.011
	Cervical 3 mm	−1231.813*	190.191	.000	−1840.812	−622.814
	Cervical 4 mm	−381.996	190.191	1.000	−990.995	227.004
	Cervical 5 mm	−46.666	190.191	1.000	−655.665	562.333
	Middle 3 mm	−704.371*	190.191	.008	−1313.370	−95.371
	Middle 5 mm	357.953	190.191	1.000	−251.047	966.952
Middle 5 mm	Apical 3 mm	−1026.721*	190.191	.000	−1635.721	−417.722
	Apical 4 mm	−357.065	190.191	1.000	−966.064	251.935
	Apical 5 mm	134.059	190.191	1.000	−474.940	743.059
	Cervical 3 mm	−1589.766*	190.191	.000	−2198.765	−980.766
	Cervical 4 mm	−739.948*	190.191	.004	−1348.947	−130.949
	Cervical 5 mm	−404.619	190.191	1.000	−1013.618	204.381
	Middle 3 mm	−1062.323*	190.191	.000	−1671.322	−453.324
	Middle 4 mm	−357.953	190.191	1.000	−966.952	251.047

Based on observed means

The error term is mean square (error) = 3,617,257.029

* The mean difference is significant at the .05 level

artifacts between solitary and neighboring implants. However, in contrast to our results, the rate of artifacts was higher in the mandible compared to the maxilla; various factors, such as differences in the device brand and variable FOVs and mAs, may explain this difference. Similar to our findings, Oliveira et al. [21] reported that the amount of artifacts varied depending on the position of the implant, with the highest rate observed in the anterior regions. These findings suggest that the GSV may vary based on the position and location of the implants. Variabilities in the density and thickness of the maxilla and mandible can justify the differences in the

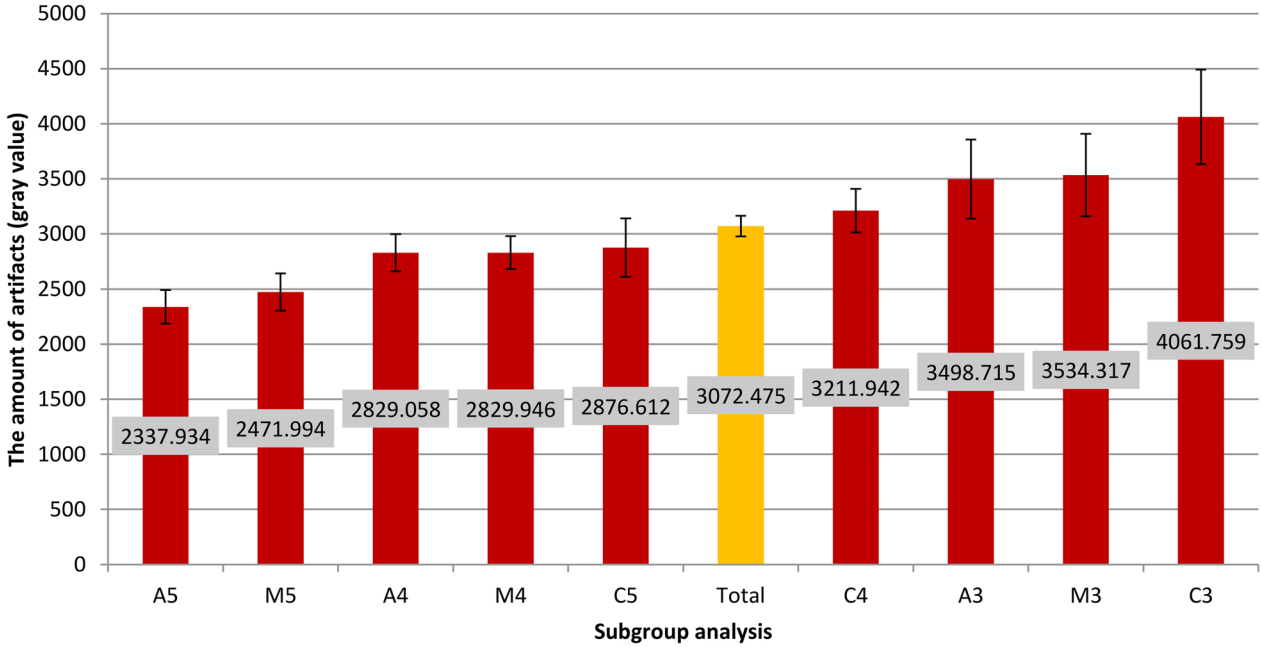

Fig. 4 Artifact value at a confidence interval of 95% (A: Apical; M: Middle; C: Coronal; 3: 3 mm from the implant; 4: 4 mm from the implant; 5: 5 mm from the implant)

Table 3 Average artifacts in different areas of both jaws

Area	The mean amount of artifacts (gray value)	SD	Number
Posterior maxilla	2612.258	2833.508	450
Anterior maxilla	3720.090	1515.503	450
Posterior mandible	2639.039	1934.081	450
Anterior mandible	3318.513	1220.341	450
Total	3072.475	2025.437	1800

number of artifacts. Evidence suggests similar objects in different anatomical positions can have different gray-scale values in CBCT images [8]. It has been shown that a single object may have different CT values in different anatomical positions, with the highest and lowest values reported in the anterior and posterior maxillary areas, respectively [8]. Moreover, Valizadeh et al. revealed that an object's position influenced the GSV of tomographic images. Comparable to the findings of this investigation, the highest rate of artifacts was attributed to the cervical one-third, probably due to prosthetic components on the implant. It is worth mentioning that titanium has a lower atomic number than metals used to fabricate prosthetic crowns, such as cobalt-chromium crowns. A higher atomic number is associated with more artifacts. Therefore, the presence of a prosthesis and titanium abutments can explain the increase in the rate of artifacts in the cervical area [22]. The quantity of metal artifacts produced by dental implants positioned in various anatomical regions within the mandible on CBCT scans was also measured by Farhangnia et al. [14]. Despite the fact that they were limited to examining mandibular scans, they discovered that metal artifacts had a more significant impact on the anterior than the posterior mandibular regions. They also found that the cervical portions produced more artifacts than the apical zone, consistent with our findings.

In agreement with the current study's findings, Vahdani et al. reported a higher contrast-to-noise ratio in the maxilla than the mandible; this difference between jaws could be attributed to variable laboratory and patient-related factors [23]. More artifact production occurs when X-rays pass through the maxilla or mandible in specific areas because they interact with the surrounding bone, teeth, and dental implants on a single plane [16]. The effect of the exomass, or the entire craniofacial area inside and outside the FOV, is another theory that could account for this variance in artifacts relative to anatomical position. Although a sizable portion of the patient's tissue attenuates X-rays, it is excluded from the resultant image [10, 18, 19, 21]. Gray value measurements in the mandible and maxilla are also impacted by nearby anatomical features, such as the spinal column and skull [18, 24].

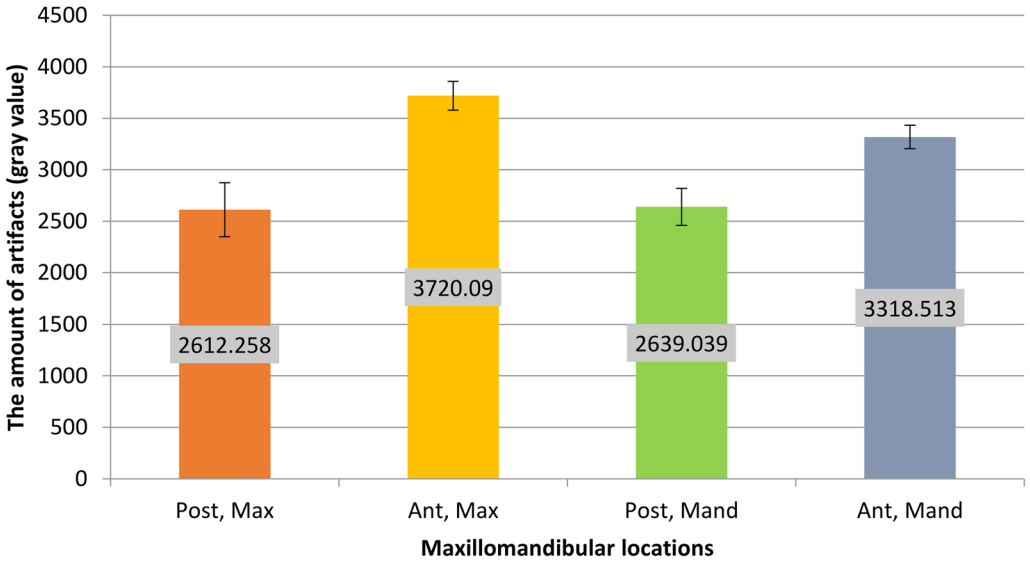

Fig. 5 A comparative chart of the average values of artifacts in different areas (*Ant* anterior, *Post* posterior, *Max* maxillary, *Mand* mandible)

A greater gray value range, or increased artifact creation, was anticipated between neighboring implants since metallic substances attenuate X-ray radiation more effectively than soft tissues and bones [25]. Nevertheless, no discernible variation was seen in the amount of artifacts surrounding solitary implants compared to those surrounding adjacent ones. This outcome could be explained by the narrow ROI specified to assess the artifacts; therefore, neighboring implants had little to no impact.

Besides, Benic et al. [10] assessed the effect of distance from the buccal surface of the implants (0.5, 1, and 2 mm) on the amount of artifacts and reported consistent results with the present study. As the distance increased, the artifact intensity was shown to significantly decrease. Fontenele et al. [9] evaluated the magnitude of artifacts generated from zirconium and titanium implants at various distances and examined their effects on the quality of CBCT images. The quantity and magnitude of artifacts in CBCT are more noticeable in areas near the implant; these findings agree with the current results. These findings indicate that increased distance from the implant decreased the artifacts' rate and the average gray value. Several other studies have investigated the relationship between distance from the implant and the rate of artifacts caused by metal implants. In line with our findings, other studies [26, 27] have also confirmed that artifacts occurred at the highest rate in the closest locations to the implant. In contrast, increasing the distance from the implant reduced the rate of artifacts. Implants generally contain metal elements in their structure with different absorption and scattering properties relative to the surrounding bone tissue, which explains the increase in the rate of artifacts and the average gray value [28].

An image artifact cannot be observed in a tomography image of an object; however, it may occur near the image generated by the reconstruction data. Artifact formation in CBCT images can be a detrimental factor in the processes of diagnosis and examination; numerous factors can influence this phenomenon. These artifacts can be intrinsic, depending on the device's quality, technology, and physical features [29], or can be related to image acquisition setting and exposure parameters, affecting the rate of artifacts [6]. Available methodologies and technologies are evolving to decrease the amount of these artifacts. It has been reported that a smaller FOV and the application of a metal artifact reduction (MAR) tool could reduce the occurrence of metal artifacts [15, 30]. The direction and tilt of the jaw are among other factors that influence the amount of artifacts; changing the jaw direction and tilt by almost 15 degrees could increase the images' quality and decrease the artifacts' rate and the duration and dose of exposure [16]. Future in vitro research must thus be developed to account for these factors when evaluating the artifacts produced by implants. Furthermore,

Table 4 Mean values of adjacent pairs

	The mean amount of artifacts (gray value)	N	SD	Standard error mean	*P* value
Pair 1					
1	3316.265	20	1411.929	315.717	0.66
2	3169.725	20	909.010	203.261	

research linking the degree of artifacts with diagnostic accuracy is necessary to determine the true degree of interference these undesired images cause in clinical practice.

Conclusions

According to the results of the present study, the magnitude and quantity of artifacts in CBCT images are affected by the anatomical location in both jaws and distance from dental implants. Artifacts were more pronounced and abundant in the upper jaw, anterior areas, and regions closer to the implant. Significantly, the anterior maxilla showed the highest rate of peri-implant artifacts, followed by the anterior mandible, while the posterior maxilla and posterior mandible indicated no significant differences. Also, the adjacent implants did not significantly influence the amount of artifacts.

Abbreviations

CBCT	Cone beam computed tomography
FOV	Field of view
kVp	Kilovoltage peak
mA	Milliamperage
GSV	Grayscale value
ROI	Region of interest
ICC	Intra- and inter-class correlation coefficients
CIs	Confidence intervals
MAR	Metal artifact reduction

Acknowledgements
The authors thank Mr. Amir Babaei for designing the graphical illustrations.

Author contributions
Y.S involved in conceptualization, methodology, software, formal analysis, investigation, data curation, writing—original draft, and visualization; S.A.M involved in formal analysis, investigation, resources, writing—original draft, writing—review and editing, and visualization; L.H involved in conceptualization, methodology, software, validation, supervision, and project administration; F.Z.B involved in methodology, formal analysis, and writing—original draft; S.S involved in conceptualization, methodology, validation, supervision, and project administration. All authors read and approved the final manuscript.

Funding
This study received no external funding.

Availability of data and materials
The datasets used and/or analyzed during the current study are available from the corresponding author upon reasonable request.

Declarations

Ethics approval and consent to participate
The study protocol was carried out in compliance with the Declaration of Helsinki and authorized by the Research Ethics Committees of the Islamic Azad University—Dental Branch, Tehran, Iran (No.: IR.IAU.DENTAL.REC.1399.090). Before participating in the study, informed consent was obtained from each participant.

Consent for publication
Not applicable.

Competing interests
There is nothing to declare.

Author details
[1]Maxillofacial Radiology Department, School of Dentistry, Shahrekord University of Medical Sciences, Shahrekord, Iran. [2]Maxillofacial Radiology Department, Faculty of Dentistry, Tehran Medical Sciences, Islamic Azad University, Tehran, Iran. [3]Department of Research Analytics, Saveetha Dental College and Hospitals, Saveetha Institute of Medical and Technical Sciences, Saveetha University, Chennai, India. [4]Student Research Committee, School of Dentistry, Shiraz University of Medical Sciences, Shiraz, Iran.

Received: 24 May 2023 Accepted: 16 January 2024
Published online: 30 January 2024

References

1. Venkatesh E, Elluru SV (2017) Cone beam computed tomography: basics and applications in dentistry. J Istanb Univ Fac Dent 51(3 Suppl 1):S102–S121
2. Lorenzoni DC, Bolognese AM, Garib DG, Guedes FR, Sant'anna EF (2012) Cone-beam computed tomography and radiographs in dentistry: aspects related to radiation dose. Int J Dent 2012:813768
3. Pauwels R, Araki K, Siewerdsen JH, Thongvigitmanee SS (2015) Technical aspects of dental CBCT: state of the art. Dentomaxillofac Radiol 44(1):20140224
4. Jacobs R, Salmon B, Codari M, Hassan B, Bornstein MM (2018) Cone beam computed tomography in implant dentistry: recommendations for clinical use. BMC Oral Health 18(1):88
5. Scarfe WC, Li Z, Aboelmaaty W, Scott SA, Farman AG (2012) Maxillofacial cone beam computed tomography: essence, elements and steps to interpretation. Aust Dent J 57(Suppl 1):46–60
6. Terrabuio BR, Carvalho CG, Peralta-Mamani M, Santos P, Rubira-Bullen IRF, Rubira CMF (2021) Cone-beam computed tomography artifacts in the presence of dental implants and associated factors: an integrative review. Imaging Sci Dent 51(2):93–106
7. Nagarajappa AK, Dwivedi N, Tiwari R (2015) Artifacts: the downturn of CBCT image. J Int Soc Prev Community 5(6):440–445
8. Schulze R, Heil U, Gross D, Bruellmann DD, Dranischnikow E, Schwanecke U et al (2011) Artefacts in CBCT: a review. Dentomaxillofac Radiol 40(5):265–273
9. Fontenele RC, Nascimento EH, Vasconcelos TV, Noujeim M, Freitas DQ (2018) Magnitude of cone beam CT image artifacts related to zirconium and titanium implants: impact on image quality. Dentomaxillofac Radiol 47(6):20180021
10. Benic GI, Sancho-Puchades M, Jung RE, Deyhle H, Hämmerle CH (2013) In vitro assessment of artifacts induced by titanium dental implants in cone beam computed tomography. Clin Oral Implants Res 24(4):378–383
11. Machado AH, Fardim KAC, de Souza CF, Sotto-Maior BS, Assis NMSP, Devito KL (2018) Effect of anatomical region on the formation of metal artefacts produced by dental implants in cone beam computed tomographic images. Dentomaxillofac Radiol 47(1):20170281
12. Alzain AF, Elhussein N, Fadulelmulla IA, Ahmed AM, Elbashir ME, Elamin BA (2021) Common computed tomography artifact: source and avoidance. Egypt J Radiol Nucl Med 52(1):151
13. Nardi C, Molteni R, Lorini C, Taliani GG, Matteuzzi B, Mazzoni E et al (2016) Motion artefacts in cone beam CT: an in vitro study about the effects on the images. Br J Radiol 89(1058):20150687
14. Farhangnia A, Reyhani Z, Farhangnia P, Hekmat B (2022) Effect of anatomical location of dental implants in the mandible on generation of metal artifacts on cone-beam computed tomography scans. Avicenna J Dent Res 14(2):63–68
15. Shokri A, Jamalpour MR, Khavid A, Mohseni Z, Sadeghi M (2019) Effect of exposure parameters of cone beam computed tomography on metal

artifact reduction around the dental implants in various bone densities. BMC Med Imaging 19(1):34
16. Luckow M, Deyhle H, Beckmann F, Dagassan-Berndt D, Müller B (2011) Tilting the jaw to improve the image quality or to reduce the dose in cone-beam computed tomography. Eur J Radiol 80(3):e389–e393
17. Song X, Li L, Gou H, Xu Y (2020) Impact of implant location on the prevalence of peri-implantitis: a systematic review and meta-analysis. J Dent 103:103490
18. Sancho-Puchades M, Hämmerle CH, Benic GI (2015) In vitro assessment of artifacts induced by titanium, titanium–zirconium and zirconium dioxide implants in cone-beam computed tomography. Clin Oral Implants Res 26(10):1222–1228
19. Pauwels R, Stamatakis H, Bosmans H, Bogaerts R, Jacobs R, Horner K et al (2013) Quantification of metal artifacts on cone beam computed tomography images. Clin Oral Implants Res 24(A100):94–99
20. Horner K, O'Malley L, Taylor K, Glenny AM (2015) Guidelines for clinical use of CBCT: a review. Dentomaxillofac Radiol 44(1):20140225
21. Oliveira ML, Tosoni GM, Lindsey DH, Mendoza K, Tetradis S, Mallya SM (2013) Influence of anatomical location on CT numbers in cone beam computed tomography. Oral Surg Oral Med Oral Pathol Oral Radiol 115(4):558–564
22. Valizadeh S, Vasegh Z, Rezapanah S, Safi Y, Khaeazifard MJ (2015) Effect of object position in cone beam computed tomography field of view for detection of root fractures in teeth with intra-canal posts. Iran J Radiol 12(4):e25272
23. Vahdani N, Moudi E, Ghobadi F, Mohammadi E, Bijani A, Haghanifar S (2020) Evaluation of the metal artifact caused by dental implants in cone beam computed tomography images. Maedica 15(2):224–229
24. Smeets R, Schöllchen M, Gauer T, Aarabi G, Assaf AT, Rendenbach C et al (2017) Artefacts in multimodal imaging of titanium, zirconium and binary titanium-zirconium alloy dental implants: an in vitro study. Dentomaxillofac Radiol 46(2):20160267
25. Cremonini CC, Dumas M, Pannuti CM, Neto JB, Cavalcanti MG, Lima LA (2011) Assessment of linear measurements of bone for implant sites in the presence of metallic artefacts using cone beam computed tomography and multislice computed tomography. Int J Oral Maxillofac Surg 40(8):845–850
26. Demirturk Kocasarac H, Koenig LJ, Ustaoglu G, Oliveira ML, Freitas DQ (2022) CBCT image artefacts generated by implants located inside the field of view or in the exomass. Dentomaxillofac Radiol 51(2):20210092
27. Bohner LOL, Tortamano P, Marotti J (2017) Accuracy of linear measurements around dental implants by means of cone beam computed tomography with different exposure parameters. Dentomaxillofac Radiol 46(5):20160377
28. Candemil AP, Salmon B, Freitas DQ, Ambrosano GM, Haiter-Neto F, Oliveira ML (2018) Metallic materials in the exomass impair cone beam CT voxel values. Dentomaxillofac Radiol 47(6):20180011
29. Esmaeili F, Johari M, Haddadi P, Vatankhah M (2012) Beam hardening artifacts: comparison between two cone beam computed tomography scanners. J Dent Res Dent Clin Dent Prospects 6(2):49–53
30. Khosravifard A, Saberi BV, Khosravifard N, Motallebi S, Kajan ZD, Ghaffari ME (2021) Application of an auto-edge counting method for quantification of metal artifacts in CBCT images: a multivariate analysis of object position, field of view size, tube voltage, and metal artifact reduction algorithm. Oral Surg Oral Med Oral Pathol Oral Radiol 132(6):735–743

Publisher's Note